A&A 469, 331–337 (2007)
DOI: 10.1051/0004-6361:20053954

Astronomy & Astrophysics

The H_α surges and EUV jets from magnetic flux emergences and cancellations

Y. C. Jiang, H. D. Chen, K. J. Li, Y. D. Shen, and L. H. Yang

National Astronomical Observatories/Yunnan Observatory, CAS, Kunming 650011, PR China
e-mail: jyc@ynao.ac.cn

Received 1 August 2005 / Accepted 1 February 2007

ABSTRACT

We analyzed multi-wavelength observations of three surges with a recurrent period of about 70 min in H_α, EUV, and soft X-ray, which occurred in the quiet-sun region on 2000 November 3. These homologous surges were associated with small flares at the same base, but their exact footpoints were spatially separated from the flare. Each surge consisted of a cool H_α component and a hot, EUV or soft X-ray component, which showed different evolutions not only in space but also in time. The EUV jets had slightly converging shapes, underwent more complicate development, showed clearly twisting structures, and appeared to open to space. The H_α surges, however, were smaller and only traced the edges of the jets. They always occurred later than the jets but had dark EUV counterparts appearing in the bright jets. These surge activities were closely associated with two emerging bipoles and their driven flux cancellations at the base region, and were consistent with the magnetic reconnection surge model. The possible cause of the delay between the surges and jets, of the dark structures in the jets are discussed, along with the possible role of flux cancellations in generation of these surges.

Key words. Sun: activity – Sun: magnetic field

1. Introduction

Jet-like dynamical phenomena in the solar atmosphere, i.e., cool or hot mass ejections, such as H_α surges (Roy 1973a), EUV, and X-ray jets (Schmahl 1981; Shibata et al. 1992a) have been observed at many wavelengths and studied for many years. The H_α surges were straight or slightly curved mass ejections stretching out and away from small flare-like brightenings at footpoints in the chromosphere into coronal heights, which moved upward at 20–200 km s^{-1}, reached heights of up to 200 000 km, and typically lasted for 10–20 min (Roy 1973a; Bruzek & Durrant 1977). They can be seen as dark features on the solar disk and usually showed a strong trend to recurrence. X-ray jets were discovered by Soft X-ray Telescope (SXT) (Tsuneta et al. 1991) aboard *YOHKOH* as transitory X-ray enhancement with apparent collimated motion. These jets are always associated with microflares or subflares occurring in X-ray bright points, emerging flux regions, or active regions, and their observational characteristics have been described in detail by Shimojo et al. (1996).

Many early observations showed that H_α surges were often correlated with EUV and X-ray emissions around their bases and that cool and hot mass ejections can be coexistent phenomena; i.e., cool and hot components can be simultaneously observed in a plasma ejection event (Rust et al. 1977; Schmahl 1981; Schmieder et al. 1988; Švestka et al. 1990; Schmieder et al. 1994). Such an association was further confirmed by the recent observations from *YOHKOH*/SXT and *Transition Region and Coronal Explorer* (TRACE; Handy et al. 1999) (Shibata et al. 1992a; Shimojo et al. 1996; Canfield et al. 1996; Alexander & Fletcher 1999; Chae et al. 1999; Asai et al. 2001; Kim et al. 2001; Yshimura et al. 2003; Liu & Kurokawa 2004). However, the detailed temporal and spatial relationships between the cool and hot ejections were not well-established. Simultaneous multi-wavelength observations of jet-like events with high resolution are needed to understand such relationships better.

Surge activities were often associated with certain types of magnetic activity around their bases in the photosphere, such as satellite polarity (Rust 1968), evolving magnetic features (Roy 1973), moving magnetic bipoles (Canfield et al. 1996). Kurokawa & Kawai (1993) found that H_α surges were often observed at the very early stage in some emerging flux regions (EFRs) and recurred for many hours. Therefore, they conclude that magnetic reconnection between a newly emerging flux and a preexisting magnetic field was the essential mechanism of H_α surge production. Shimojo et al. (1998) also report that most X-ray jets favor regions of evolving magnetic flux (increasing or decreasing) and occur at the mixed polarity regions in the periphery of sunspots. More recently, Chae et al. (1999), Yoshimura et al. (2003), and Liu & Kurokawa (2004) show that surges and jets are closely correlated with magnetic flux cancellations at their footpoints, forced by the newly emerging flux with a preexisting ambient field. These observations support the magnetic reconnection surge model (Rust 1968; Roy 1973a; Shibata et al. 1992a; Schmieder et al. 1995; Canfield et al. 1996, and the references therein). Shibata et al. (1992a), Yohoyama & Shibata (1995), and Yohoyama & Shibata (1996) show in their two-dimensional MHD numerical simulations that magnetic reconnection between emerging magnetic fluxes and preexisting fields actually produce adjacent hot (X-ray) and cold (H_α) plasma ejections simultaneously. Detailed investigations of the magnetic field evolution during surges will provide an insight into the reconnection model and could help in understanding the generation mechanism of surges.

On 2000 November 3, three surge activities repeatedly occurred in the quiet-sun to the north of NOAA AR 9213 (N03W05), and the first jet was preliminarily reported by

David McKenzie in SXT *science Nugget* of 10 November 2000. In our paper, we present H_α, EUV, soft X-ray, and photosphere magnetic field observations of the three surges at length. We show that these surges were an obvious result of the cancellation between emerging bipoles and the preexisting magnetic field. We further show that these observations may serve as evidence of the magnetic reconnection in the course of these surges. For convenience, we use the traditional term "surge", and "jet" refers to the cool and hot plasma ejections throughout this paper.

2. Observations

The observations used in the present study include:

1. Full-disk H_α images from the global H_α five-station network (Steinegger et al. 2000). The stations are Big Bear Solar Observatory (BBSO) in the USA, Kanzelhohe Solar Observatory in Austria, Catania Astrophysical Observatory in Italy, Yunnan Astronomical Observatory and the Huairou Solar Observing Station in China. The observations at BBSO covered the three surges well. The cadence was 1 min, and the pixel size of the H_α images is roughly 1″, which yields a spatial resolution of 2″.
2. TRACE Fe IX/X 171 Å (1×10^6 K) images with a cadence of 1 min and a pixel size of 0.″5 (Handy et al. 1999).
3. SXT full-disk soft X-ray images in the wavelength range of 3–50 Å ($2–4 \times 10^6$ K) with a varying cadence and a pixel resolution of 4.9″ (Tsuneta et al. 1991).
4. High-resolution longitudinal magnetograms and continuum intensity images with a cadence of 1 min and a pixel size of 0.″625 from the Michelson Doppler Imager (MDI) onboard the *Solar and Heliospeheric Observatory* (SOHO) (Scherrer et al. 1995). On 2000 November 3, MDI observations in high-resolution mode started at 16:37 UT when the first surge was in process. The full-disk MDI magnetograms with a spatial resolution of 2″ per pixel and a cadence of 96 min are also examined.
5. Full-disk Fe XII 195 Å images from the Extreme-ultraviolet Images Telescope on SOHO (SOHO/EIT) with a cadence of 12 min and a pixel size of 2.6″ (Delaboudiniére et al. 1995).

3. H_α surges and EUV jets

From 16:30 to 19:00 UT on 2000 November 3, three major surges recurred with a period of about 70 min in the quiet-sun region to the north of NOAA AR 9213 (N03W05). Figures 1a, 1b, and 1c present H_α image, soft X-ray image, and a MDI magnetogram of the surge region, respectively, and Fig. 1d shows their general appearances in EIT 195 Å observations. It is clear that all of these surges were ejected from the same site, which showed up as a bright plage patch in the H_α image and as mixed polarities region in MDI magnetogram. Below we show that new flux emergences and flux cancellations occurred in this region.

3.1. Morphologic evolution

Figures 2–4 respectively show the morphologic evolutions of the first, second, and third surges in BBSO H_α, TRACE 171 Å, or SXT soft X-ray. While all of these surges were well covered by BBSO H_α observations, only the first surge was observed by YOHKOH/SXT, and the early stage of the first jet and the ending stage of the second jet were lost in EUV due to data gaps from 16:17 to 16:36 UT and from 17:53 to 18:12 UT for TRACE

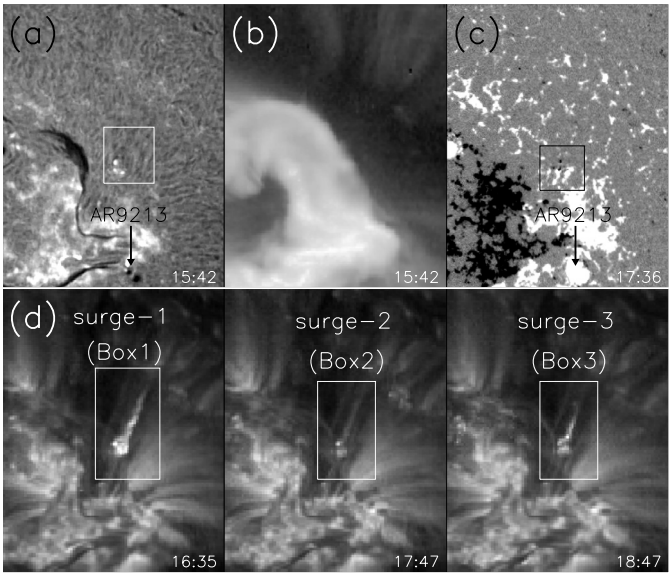

Fig. 1. The appearance of the surge region in BBSO H_α image **a)**, SXT soft X-ray image **b)**, MDI magnetogram **c)**, and the three recurrent jets in EIT 195 Å images **d)**. The field of view (FOV) is $500'' \times 640''$. The black window in the magnetogram indicates the FOV of Fig. 6, and the areas in the Box1, Box2, and Box3 represent the FOVs in Figs. 2–4, respectively.

observations. These plasma eruptions had the most obvious appearances in 171 Å images. They were nearly straight, mainly bright features with embedding dark structures. Like situations found in the H_α surge by Kurokawa & Kawai (1993) and in soft X-ray jets by Shibata et al. (1994), they showed triangular shapes and slightly curved to the west. In the H_α images, these surges showed as slightly curved dark features with a smaller dimension than in EUV. The first jet also showed as a bright line structure in SXT soft X-ray, which was already visible at 16:37 UT after a YOHKOH night and showed the nearly same timing, location, and appearance as the 171 Å jet. It is noted that an early EUV jet spurted out from the same base before 16:16 UT (see the images at 16:10 and 16:15 UT in Fig. 2b), but we do not know whether this jet was the early stage of the first jet due to the data gap of about 20 min in TRACE observations after 16:17 UT. Therefore, the first jet started before 16:37 UT, but its precise start time was unknown. As noticed by McKenzie in the SXT nugget-type report, these jets seem to eject outward along preexisting open field lines, so were open to space. When the clumpy plasma was channeled and moved outward along the open field lines, the jet paths changed shape and some helical and twisting structures were observed.

3.2. Relationship between jets and flares

As a fairly common characteristic of jets, these plasma ejections were all accompanied by small flares, i.e., subflares or microflares, at the same base. The small flares were obvious in H_α and 171 Å for the three jets, and also in soft X-ray for the first jet. The H_α light curves in the area containing these small flares (indicated by the white box in H_α image in Fig. 1 and black boxes in Figs. 2–4) are measured and plotted in Fig. 5a. We see that the H_α emission enhancements peaked at around 16:37, 17:45, and 18:52 UT, and that there were corresponding small fluctuations in GOES soft X-ray flux (also shown in Fig. 5a) relative to the smooth background flux. In soft X-ray, the small flare during the

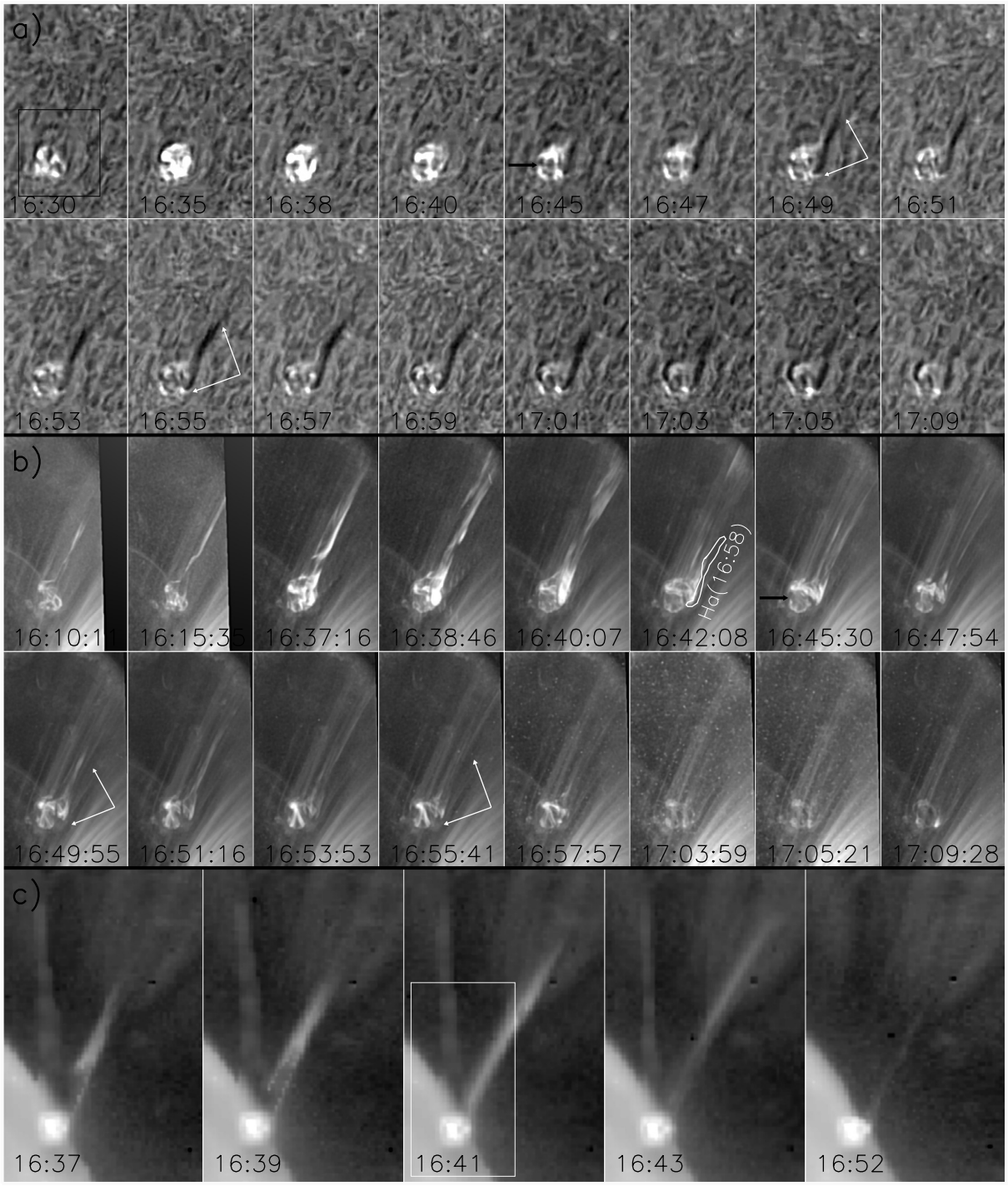

Fig. 2. BBSO H_α **a)**, TRACE 171 Å **b)**, and YOHKOH soft X-ray **c)** images showing the evolution of the first surge. The FOV in **a)** and **b)**, indicated by the Box1 in Fig. 1, is 145″ × 250″. The FOV in **c)** is 280″ × 440″, and the area in the white box shows the FOV in **a)** and **b)**.

first jet was a bright patch without an obvious substructure. In 171 Å, however, the brightenings in the base region of all three jets clearly consisted of two parts separated by EUV emission gaps. One was the exact footpoints of the jets, and the other the loop-like brightenings of the small flares. Such disconnectivity suggests that the jets were spatially separated from the bright flare loops. Similar situations in X-ray jets were also discussed by Shibata et al. (1994), Shimojo et al. (1996), and Canfield et al. (1996). More interestingly, the two-part EUV brightenings at the base region had obvious chromospheric counterparts, which can be easily distinguished as two bright patches in H_α images. In Figs. 2–4, the gaps between the two brightening parts are indicated by the black arrows in the 171 Å images at 16:45, 17:45, and 18:47 UT, and in H_α images at 16:45, 17:49, 18:47 UT, respectively.

3.3. Relationship between jets and surges

A more striking characteristic of the three plasma ejections, however, is that the occurrence and appearances of the H_α dark surges (the cool components) were clearly different from the EUV or soft X-ray bright jets (the hot components), not only

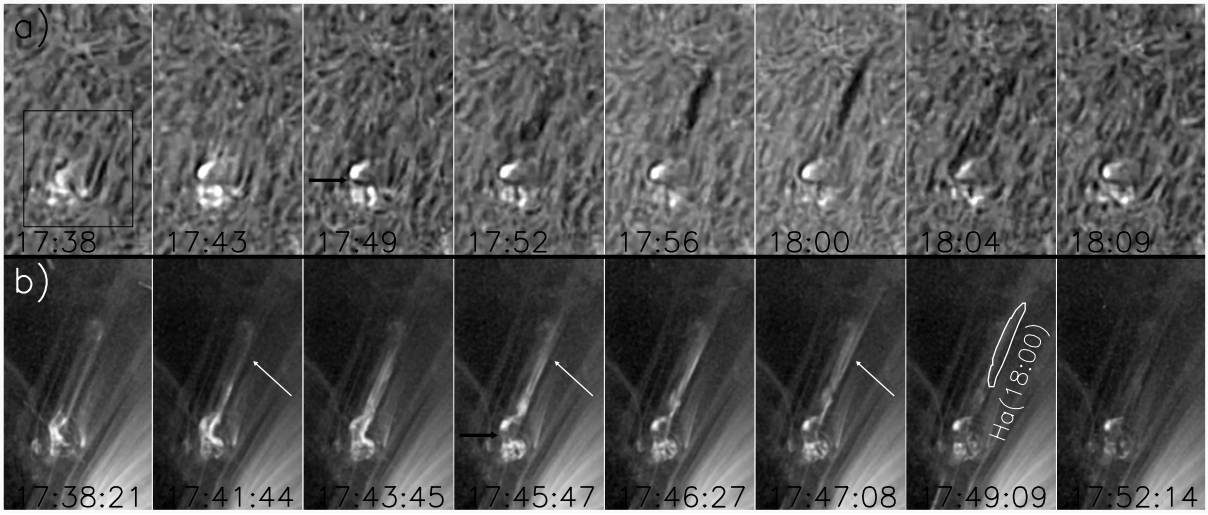

Fig. 3. BBSO H_α **a)** and TRACE 171 Å **b)** images showing the evolution of the second surge. The FOV, indicated by the Box2 in Fig. 1, is $130'' \times 220''$.

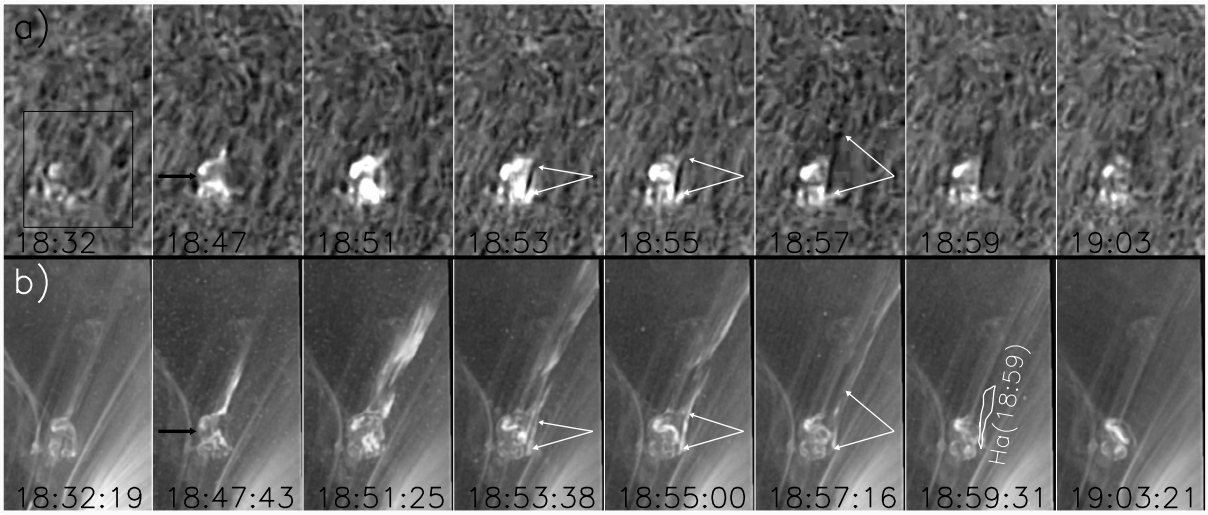

Fig. 4. BBSO H_α **a)** and TRACE 171 Å **b)** images showing the evolution of the third surge. The FOV, indicated by the Box3 in Fig. 1, is $130'' \times 220''$.

in space but also in time. In the first event, the EUV jet started to occur before 16:37 UT, reached the maximum length of 2.21×10^5 km at around 16:43 UT, then quickly faded away and completely disappeared after about 16:53 UT. The H_α surge, however, first appeared by 16:40 UT, and reached the maximum length of 6.64×10^4 km at around 16:58 UT when the EUV jet had disappeared. Moreover, the paths of the hot and cool components were possibly along different field lines. In Fig. 2, the H_α surge near its maximum phase was superposed on the 171 Å image at 16:42. It is clear that the H_α surge was shorter and thinner than the bright 171 Å jet and only traced its western edge. After the occurrence of the H_α surge, its EUV counterpart was a region with weak darkening (indicated by the white arrows) as compared with the earlier 171 Å images. During the second and third events, the H_α surges and the EUV jets showed similar spatial and temporal relationships. In Fig. 3 for the second event, the H_α surge with the maximum length at 18:00 UT was superposed on the EUV image at 17:49 UT. The spatial difference between the H_α surge and bright EUV jet is clear. In this case, however, it is noted that the H_α surge was cospatial with a preexisting dark EUV structure (indicated by the white arrows) inside the bright jet. At the beginning of the third H_α surge, a bright EUV structure appeared at the site of the surge (indicated by the white arrows) and then became a dim region by 18:59 UT. The H_α surge reached its greatest length of 4.57×10^4 km at 18:59 UT and was very small compared to the 171 Å jet, which ejected out of the field of view (FOV) of TRACE after 18:53 UT. In Fig. 4, the H_α surge at 18:59 UT was superposed on the EUV image at the same time. Again, the H_α surge was located at the bright western edge of the 171 Å jet. In Table 1, the temporal relationship between the cool and hot components of the three surges is summarized. In Fig. 5b, the projected lengths of the three surges and jets in H_α and EUV or soft X-ray are plotted. Since the EUV jets during the first and third events were ejected out of the TRACE FOV, the lengths of the first jet we measured according to the SXT observations; and for the third event, only the lengths of the 171 Å jet inside the TRACE FOV are given. For all of three events, the cool components obviously showed different temporal behavior from their hot counterparts. The first appearances and the maximum length phase of the cool components were later than that of their hot counterparts, and the delay intervals of the maximum length phase between the hot and cool

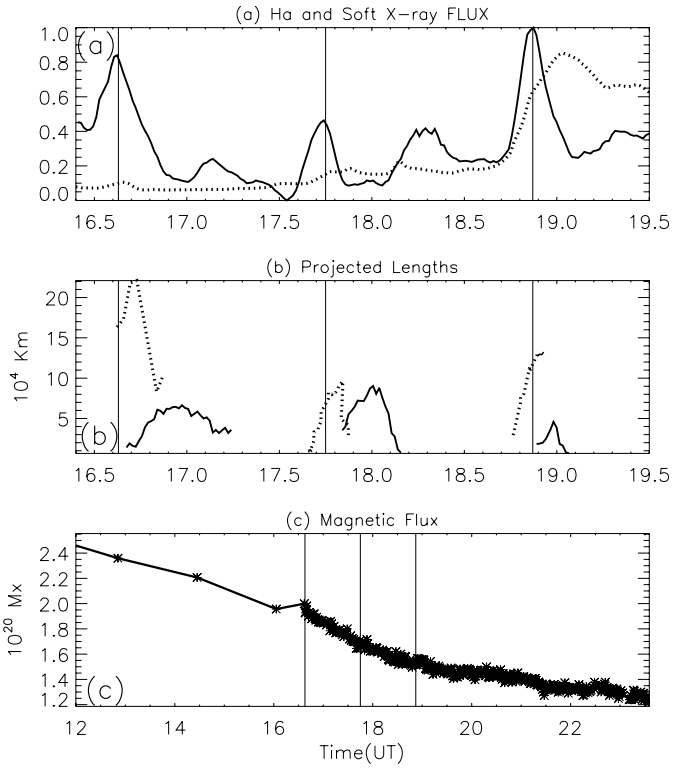

Fig. 5. a) H_α light curves as the function of time in the area containing the three small flares (solid line), which are computed from the intensity, integrated and normalized over the area, and time profiles of GOES-8 soft X-ray in the energy channel of 1–8 Å (dashed line), which are displayed in an arbitrary unit to fit in the panel. **b)** Projected lengths of the surges in H_α (solid line) and of the jets in EUV or soft X-ray (dashed line). **c)** Changes in the positive magnetic flux in the black box in Fig. 6. The solid vertical bars indicate the maximum times of the three small flares.

components were 15, 10, and 6 min for the first, second, and third surges, respectively. The hot components appeared around the peak times of the associated small flares, while the cool components appeared after the peak times, which is consistent with the result of Schmieder et al. (1995). It is noted that, however, all of the H_α surges had corresponding EUV dim region or dark structures.

4. Magnetic flux emergence and cancellation

Figure 6 shows the evolution of longitudinal magnetic fields in the surge foot region in the photosphere. By carefully examining high-resolution and full-disk MDI magnetograms, three conspicuously emerging bipoles were identified around a preexisting positive magnetic patch, "P", in this region, and their preceding (positive) and following (negative) poles were labeled as "p1", "p2", "p3", "n1", "n2", and "n3", respectively. As a normal phenomenon associated with emerging bipole, the positive and negative poles showed a separating motion after their first emergences. The n1 first appeared at 03:12 UT, and the p1 emerged close to the P with same polarity and then separated from it. Due to the n1 emergence preceding the surges by about 13 hours and due to the lack of direct interaction between the n1 and the P, it seems that the p1-n1 bipole emergence was not directly associated with the surges we studied here. The p2 and n2 showed their earliest signals as small magnetic patches at around 08:03 and 12:51 UT, respectively. Different from the n1 emergence, the n2 directly popped out from a positive flux background of the P. Due to the spreading motion, it was then driven to collide and cancel with the P.

Such flux cancellation obviously persisted throughout the journey of the bipole emergence until the n2 completely disappeared at about 23:00 UT. As a result, the area and the flux of the n2 were smaller than that of the p2 all along so the p2 eventually showed up as a pore (see the MDI intensity image at 23:30 UT) while the n2 did not. It is possible that this bipole emerged symmetrically and simultaneously, but the n2 had no sooner presented then it cancelled with the P, which led to its first appearance being later than that of the p2. Therefore, it seems that we can reasonably take 08:03 UT as the start time of the p2-n2 bipole emergence. Since the flux cancellation continued throughout the duration of the surge activities, we believe that the n2-p2 bipole emergence and the forced flux cancellation were closely related to these surges. The third bipole was smaller than the first and second bipoles. Its two poles, the p3 and n3, first appeared simultaneously at around 17:30 UT. Similar to the n2, the n3 emerged to the west of the P and was then forced to collide and cancel with the P due to the spreading motion. The flux cancellation between the n3 and P was clearly manifested by making a comparison between the magnetograms at 17:32 and 23:30 UT. We see that a positive tongue of the P was gradually eroded and became smooth by 23:30 UT (indicated by the arrows in the two magnetograms). Since the n3-p3 bipole emerged after the end of the first surge but just before the start of the second surge, we believe that this emergence and its driven flux cancellation were closely associated with the second and third surges.

As a result of continuous flux cancellation with both the n2 and n3, flux in the P was substantially lost. This can be directly seen from its decreasing area in a series of MDI magnetograms. In Fig. 6, it is seen that the EUV flares and jets were very close to the P, showing a close association between the jet activities and the flux cancellation. The changes in the positive flux in an area containing the P from 12:00 to 23:00 UT were measured and plotted in Fig. 5c. It is clear that the flux in P continuously decreased, from 2.45 to 1.25×10^{20} Mx between 12:00 and 23:00 UT with an average flux-loss rate of 3.0×10^{15} Mx s^{-1}. From 16:37 to 19:00 UT during which the surges occurred, however, the flux decreased from 1.95 to 1.5×10^{20} Mx. This gives a higher average flux-loss rate of 5.2×10^{15} Mx s^{-1}, implying a relatively quick flux cancellation in the course of the surge activities. Thus, it seems that the second and third emerging bipoles and their driven flux cancellation played a central role in producing the surge activities.

5. Conclusions and discussions

By means of BBSO H_α, TRACE EUV, and SXT soft X-ray observations, as well as MDI magnetograms, the morphologic, and dynamic characteristics of the three surge activities were described, and the associated evolution of photosphere magnetic field examined. Our main results are summarized as the following points. (1) The three surges occurred intermittently with a recurrent period of about 70 min. They originated in the same base and seem to be open to space. Each surge was accompanied by a small flare, but its exact footpoint was spatially separated by voids from the associated flare. (2) The EUV jets underwent more complicate development and had more structures than the H_α surges. They showed helical and twisting structures and had slightly converging shapes, while the H_α surges were smaller and only traced their edges. The appearances of the hot

Table 1. Temporal relationship between the cool and hot components of the three surges.

Events	First event		Second event		Third event	
	Hot	Cool	Hot	Cool	Hot	Cool
Lifetime (Min)	>16	~34	>13	~19	~10	~10
First Appearance (UT)	before 16:37	16:40	17:39	17:50	18:45	18:53
Delay interval (Min)	>3		~11		~8	
Maximum Length	16:43 UT	16:58 UT	17:50 UT	18:00 UT	18:53 UT	18:59 UT
(10^4 km)	22.10	6.64	9.61	9.03	13.25	4.57
Delay interval (Min)	~15		~10		~6	
Subflare maximum	16:37 UT		17:45 UT		18:52 UT	

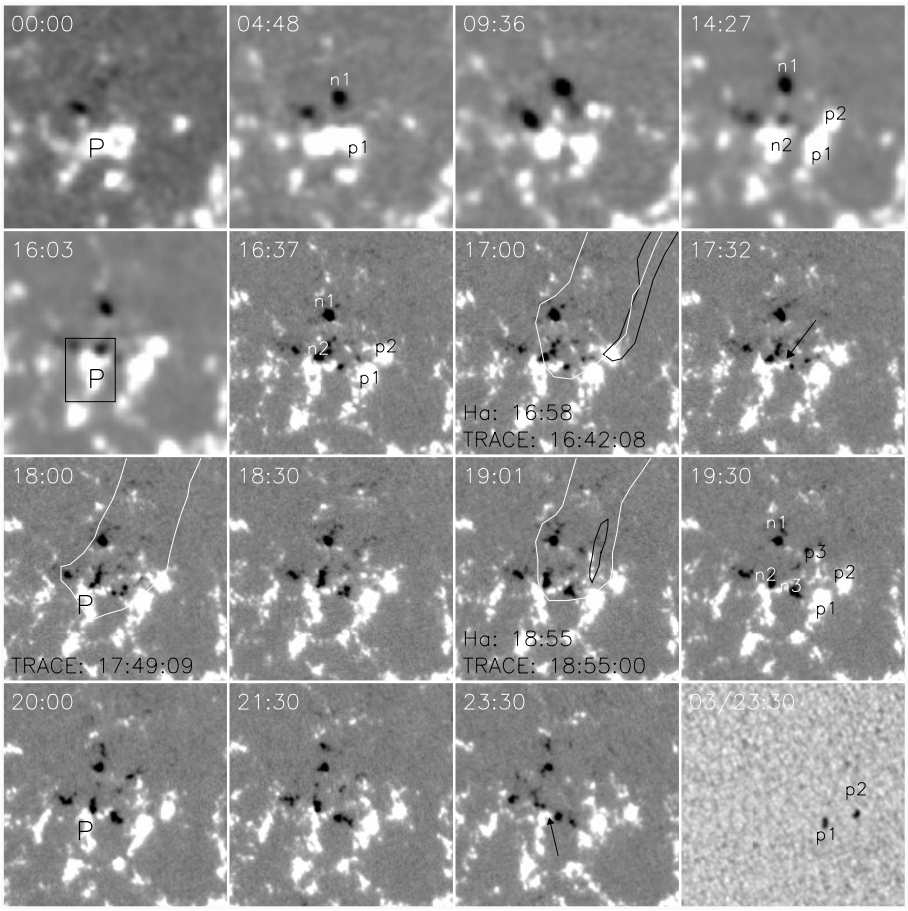

Fig. 6. MDI magnetograms showing the evolution of magnetic field around the base region of the surges. To aid matching, the last frame presents an MDI intensity image, and the outlines of the H_α surges and the EUV jets (including the small flares) in the three events are superposed as black and white contours, respectively. The black box indicates the area in which the changes of the positive flux are measured and plotted in Fig. 5c. The positive and negative poles of the three emerging bipoles are denoted as "p1", "p2", "p3", "n1", "n2", and "n3". The FOV, indicated by the black box in Fig. 1, is $100'' \times 100''$.

and cool components were not simultaneous. The cool components always occurred later than the hot components, and were associated with weak dim area or dark structures in the hot components. (3) These surges clearly resulted from the two distinctly emerging bipoles and their forced flux cancellations around the base region before and during the surge activities.

Many aspects of these observations can be explained by magnetic reconnection between the preexisting open fields and the newly emerging fields. Flux cancellation driven by the emerging bipoles can be considered as a slow reconnection in the lower atmosphere (Wang & Shi 1993; Jiang & Wang 2000, 2001). The occurrence of the associated small flare and the converging shapes of the EUV jets, as well as the gaps between their footpoints and the loop-like flare brightenings, can be regarded as evidence of magnetic reconnection in these jets (Shibata 1998). The twisting structures in the EUV jets can also be attributed to the relaxation of a stored twist as a result of reconnection between closed twisted new flux tubes and untwisted surrounding coronal field (Shibata & Uchida 1986; Schmieder et al. 1995; Canfield et al. 1996). The coexisting, but different, paths of the cool and hot components were consistent with the 2D MHD numerical simulations of the reconnection model of Yohoyama & Shibata (1996), in which both cool and hot plasma can be ejected along separate magnetic fields and must be dynamically connected to each other.

During surge activities, delay in the peak emission of hot and cool plasma were not uncommon. Schmieder et al. (1994) find a delay of 3–4 min between cool and hot plasma emission, and Alexander & Fletcher (1999) show that the maximum extent time of an X-ray jet precede that of in EUV by 5 min and they explain such a delay being caused by the cooling of the earlier, hotter jet material. In the case studied here, the H_α surges were observed before as bright structures in EUV in the first and third events; thus, we could conclude that their appearances were the results of cooling hot plasma, and the cooling time was about 6–15 min as mentioned in Sect. 3.3. It is well known that the coronal emission of the jet is absorbed by the Lyman continuum of helium (Mein et al. 2001; Schmieder et al. 2004;

Anzer & Heinzel 2005). In the bright EUV jet during the second events, we clearly see that dark structures appear at the location of a future surge. It means that the cool material still exists, but its optical thickness is not enough to be visible in H_α or the spatial resolution of TRACE EUV observations is better than that of H_α on the ground. That we see dark absorbed structures in the EUV jets means that these cool structures are located between the coronal emission and the observer, and the EUV jets are less inclined than the surges to the observer.

The new flux emergences and the forced flux cancellations contain the key elements that are needed to produce these surge activities. Chae (1999) propose a two-step reconnection model, in which flux cancellation is the direct result of slow magnetic reconnection in the lower atmosphere. More recently, Fletcher et al. (2001) in their three-dimensional potential field model demonstrate that small-scale flux cancellation in the photosphere can cause field lines to open at a different location that the cancellation so lead to TRACE ejecta. We think that these models contain the basic aspects of a surge mechanism that can tie together the slow flux cancellation in the photosphere with the quick surge activities in the chromosphere and corona. In our case, the recurrent period of the homologous jets was only about 70 min. As noticed by Kim et al. (2001), this is much shorter than that of homologous flares, thus helicity injection by emerging flux or self-helicity generation by reconnection of small-scale flux tubes is possibly important in producing these homologous jets. Finally, we would like to point out that an extended study is needed to examine the occurrence of surge at the very early stage of new flux emergences by means of round-the-clock observations, such as H_α data from the five-station global H_α network.

Acknowledgements. We thank the referee B. Schmieder for many constructive suggestions. We are grateful to the observing staff at BBSO for making good observations and to the YOHKOH team, the TRACE, the EIT, and MDI teams for data support. The work is supported by the NSFC under Grants 10573033 and 40636031 and by the National Key Research Science Foundation (2006CB806303).

References

Alexander, D., & Fletcher, L. 1999, Sol. Phys., 190, 167
Anzer, U., & Heinzel, P. 2005, ApJ, 622, 714
Asai, A., Ishii, T. T., & Kurokawa, H. 2001, ApJ, 555, L65
Brueckner, D. E., Howard, R. A., Koomen, M. J., et al. 1995, Sol. Phys., 162, 357
Bruzek, A., & Durrant, C. J. 1977, Illustrated Glossary for Solar and Solar-Terrestrial Physics, Astrophysics and Space Science Library (Dordrecht: Reidel), Vol. 69
Canfield, R. C., Peardon, K. P., Leka, K. D., et al. 1996, ApJ, 464, 1016
Chae, J. 1999, in ASP Conf. Ser., 19th NSO/SP International Workshop on High-Resolution Solar Physics: Theory, Observations, and Techniques, ed. T. Rimmele, K. S. Balasubramaniam, & R. Radick (San Francisco: ASP)
Chae, J., Qiu, J., Wang, H., et al. 1999, ApJ, 513, L75
Delaboudiniére, J.-P., Artzner, G. E., Brunaud, J., et al. 1995, Sol. Phys., 162, 291
Fletcher, L., Metcalf, T. R., Alexander, D., et al. 2001, ApJ, 554, 451
Handy, B. N., Acton, L. W., Kankelborg, C. C., et al. 1999, Sol. Phys., 187, 229
Jiang, Y., & Wang, J. 2000, A&A, 356, 1055
Jiang, Y., & Wang, J. 2001, A&A, 367, 1022
Kim, Y.-H., Kim, K.-S., & Jang, M. W. 2001, Sol. Phys., 371, 379
Kurokawa, H., & Kawai, G. 1993, in The Magnetic and Velocity Fields of Solar Active Region, ed. H. Zirin, G. Ai, & H. Wang (San Francisco: ASP), ASP Conf. Ser., 46, 507
Liu, Y., & Kurokawa, H. 2004, ApJ, 610, 1136
Mein, N., Schmieder, B., DeLuca, E. E., et al. 2001, ApJ, 556, 438
Roy, J. R. 1973, Sol. Phys., 28, 95
Rust, D. M. 1968, in Structure and Development of Solar Active Regions, ed. K. O. Kiepenheuer (Dordrecht: Reidel), IAU Symp., 35, 77
Rust, D. M., Webb, D. F., & Mac Combie, W. 1977, Sol. Phys., 54, 53
Scherrer, P. H., et al. 1995, Sol. Phys., 162, 129
Schmieder, B., Simnett, G. Mein, P., & Tandberg-Hanssen, E. 1988, A&A, 201, 327
Schmieder, B., Golub, L., & Antiochos, S. K. 1994, ApJ, 425, 326
Schmieder, B., Van Driel-Gesztelyi, L., & Freeland, S. 1995, Sol. Phys., 156, 245
Schmieder, B., Lin, Y., Heizel, P., & Schwartz, P. 2004, Sol. Phys., 221, 297
Schmahl, E. J. 1981, Sol. Phys., 69, 135
Shibata, K. 1998, in Proc. of the International Meeting on Jets, Solar Jets and Coronal Plumes, ed. T.-D. Guyenne, 137, ESA SP-421
Shibata, K., & Uchida, Y. 1986, Sol. Phys., 103, 299
Shibata, K., Ishido , Y., Acton, L. A., et al. 1992a, PASJ, 44, L173
Shibata, K., Nozawa, S., & Matsumoto, R. 1992b, PASJ, 44, 265
Shibata, K., Nitta, N., Strong, T., et al. 1994, ApJ, 431, L51
Shimojo, M., Hashimoto, S., Shibata, K., et al. 1996, PASJ, 48, 123
Shimojo, M., Shibata, K., & Harvey, K. L. 1998, Sol. Phys., 178, 379
Steinegger, M., et al. 2000, in Proc. 1st SOLSPA Euroconference, The Solar Cycle and Terrestrial Climte, ESA SP-463, 617
Švestka, Z., Fárník, F., & Tang, F. 1990, Sol. Phys., 127, 149
Tsuneta, S., et al. 1991, Sol. Phys., 136, 37
Wang, J., & Shi, Z. 1993, Sol. Phys., 143, 119
Yokoyama, T., & Shibata, K. 1995, Nature, 375, 42
Yokoyama, T., & Shibata, K. 1996, PASJ, 48, 353
Yoshimura, K., Kurokawa, H., & Shine, R. 2003, PASJ, 55, 313